HOW DIPOLE-DOMINANT IS GANYMEDE'S CORE FIELD? Alain M. Plattner[1], Alyssa C. Mills[1], Catherine L. Johnson[2,3], [1]Dept. of Geological Sciences, University of Alabama, Tuscaloosa, AL 35487, USA, amplattner@ua.edu. [2]Dept. of Earth, Ocean and Atmospheric Sciences, University of British Columbia, Vancouver, BC, V6T 1Z4, Canada. [3]Planetary Science Institute, Tucson, AZ 85719, USA

Introduction

Based on Galileo satellite magnetic data collected between 1996 and 2000, Ganymede's core magnetic field had been described as strongly dipolar ([1]). This conclusion led to discussions that Ganymede's core magnetic field may be generated within a very small active dynamo region deep inside Ganymede's interior, at a radial position of possibly only $\sim 200\,\mathrm{km}$ ([1]). [2] confirmed the magnetic field description of [1] using the data collected by the Juno satellite flyby on June 7th, 2021. The strong dipole dominance of the magnetic field model by [1] and thus the extremely-deeply seated magnetic source led to discussions and development of dynamo models that could create such a magnetic field (e.g. [3, 4, 5])

The limited spatial coverage of the Galileo tracks (Fig. 1), together with data uncertainties, may give rise to alternative magnetic field models with substantially different properties. Here, we assess this possibility by constructing a range of different models that fit the flyby data similarly well.

Limitations of Data Coverage

Internal planetary magnetic fields $\boldsymbol{B}$ are typically described as linear combinations of spherical harmonics

$$V(r,\theta,\phi) = R\sum_{l=1}^{L_{\max}}\sum_{m=0}^{l}(g_{l,m}\cos m\phi + h_{l,m}\sin m\phi)\cdot \cdot\left(\frac{R}{r}\right)^{l+1} P_{l,m}(\cos\theta) \quad (1)$$

$$\boldsymbol{B}(r,\theta,\phi) = -\nabla V(r,\theta,\phi), \quad (2)$$

where V is the magnetic potential, r, θ, ϕ are the radial, colatitudinal, and longitudinal coordinates, R is the planetary body's radius, l and m are the spherical-harmonic degree and order, $L_{\max}$ is the maximum spherical-harmonic degree, $P_{l,m}$ are Legendre polynomials normalized as in [1], and $g_{l,m}$ and $h_{l,m}$ are coefficients describing a model for the internal magnetic field.

Solving for $g_{l,m}$ and $h_{l,m}$ (eq. 1) from magnetic data $\boldsymbol{B}$ (eq. 2) with only limited spatial coverage leads to correlations between the spherical-harmonic coefficients (see e.g. [6], their Fig. 5.3). For the data locations of Galileo and Juno (location data from NAIF [7], processed using SpiceyPy [8]), the limited spatial coverage causes $g_{1,0}$ to be strongly correlated with coefficients of degrees $l \geq 2$ (Fig. 2). As a consequence, the available data can not distinguish between signal strength in $g_{1,0}$ versus in the higher-degree coefficients that are correlated with $g_{1,0}$.

In their magnetic-field model, [1] used only G1, G2, and G28 (Fig. 1), because flybys G7 and G29 were at substantially higher altitudes. To demonstrate that the issue of limited coverage persists, we included all Galileo Ganymede flyby tracks except for G8 (not shown in Fig. 1), which occurred when Ganymede was inside Jupiter's current sheet ([1]).

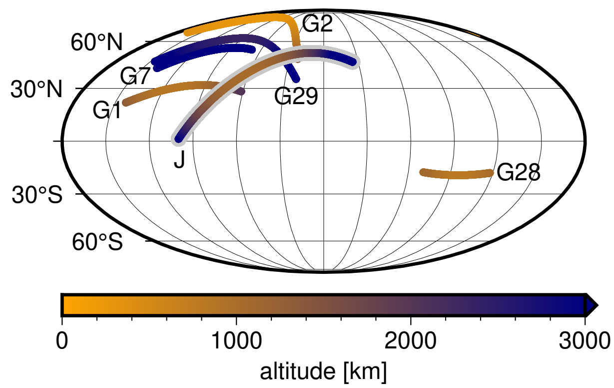

Figure 1: Galileo and Juno (gray outline) tracks. Altitude is above mean Ganymede radius $2631.2\,\mathrm{km}$. Projection is Mollweide, centered on Ganymede's sub-Jupiter point. Ganymede's leading hemisphere is on the left.

Construction of Alternative Core Field Models

To demonstrate the limitations of available data coverage, we calculated a range of magnetic field models that fit the data at least as well as the solutions of [1] (rms error $13.7\,\mathrm{nT}$) and [2] (rms error $7.8\,\mathrm{nT}$ without Juno, and $8.3\,\mathrm{nT}$ with Juno data). We calculated our models by solving for coefficients with maximum spherical-harmonic degree $L_{\max} = 3$ and by prescribing values for $g_{1,0}$. Because of the strong correlation of $g_{1,0}$ with other spherical-harmonic coefficients (Fig. 2), the correlated coefficients can compensate for our choice of $g_{1,0}$, leading to higher power in the quadrupole (spherical-harmonic degree 2) and octupole (degree 3) components of the resulting magnetic-field models (Table 1).

Like [1] and [2], we subtracted Jupiter's background field from the data and additionally solved for a uniform field for each track, together with the spherical-harmonic

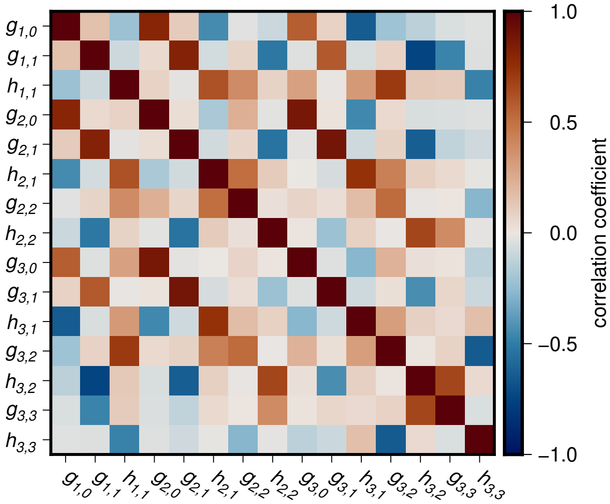

Figure 2: Correlation between the spherical-harmonic coefficients when solving for $g_{l,m}$ and $h_{l,m}$ in eq. (1) from magnetic data (eq. 2) given along the tracks in Fig. 1, including Juno's track.

coefficients. Because the magnetic data of Juno's flyby were not available on the planetary data system at the time of writing, our magnetic field models (Table 1) are solely based on Galileo data. Our correlation analysis (Fig. 2) included the Juno flyby, because correlation only depends on data location and not data values. Correlation analysis with and without the Juno flyby yielded similar results. We thus expect a similar range of models once the Juno flyby magnetic data become available.

The coefficients $g_{l,m}$ and $h_{l,m}$ allow for estimating a source radial position r_s and thus depth ($r_{\text{planet}} - r_s$) to the magnetic source, such as a magnetic dynamo. [1] used a method based on the ratio between the quadrupole and dipole power (q/d in Table 1), given as the sum of squares of coefficients for $l = 2$ divided by the sum of squares of coefficients for $l = 1$. We calculated r_s (Table 1) based on the method of [9]. The spatial pattern of the resulting magnetic field models I and II appear to be similarly plausible examples of core magnetic fields (Fig. 3).

Model	prescribed $g_{1,0}$	rms	q/d	r_s
I	–	11 nT	0.004	350 km
II	−700 nT	4 nT	0.007	1120 km
III	−1000 nT	7 nT	0.12	1870 km

Table 1: Three models fitting the data to a similar extent. Model I was constructed for $L_{\max} = 2$ and using tracks G1, G2, G28, with no prescribed $g_{1,0}$. The resulting $g_{1,0}$ value was -735 nT. Models II and III were constructed using tracks G1, G2, G7, G28, G29 and $L_{\max} = 3$ with prescribed $g_{1,0}$. Residual rms was calculated over tracks G1, G2, G28.

Discussion and Conclusions

Presently-available Ganymede magnetic field data can not uniquely constrain Ganymede's core magnetic field and the depth to the magnetic source region. Our models yielded source radii r_s between 300 km and 1900 km.

To be able to constrain the magnetic source depth, we require data coverage over a broader area of Ganymede's surface. Future Juno flybys will help constrain the models by reducing correlation between the spherical-harmonic coefficients. The upcoming JUpiter ICy moons Explorer (JUICE) satellite mission carrying a magnetometer is set to orbit Ganymede in the early 2030s and will substantially improve constraints on the depth to Ganymede's internal magnetic sources.

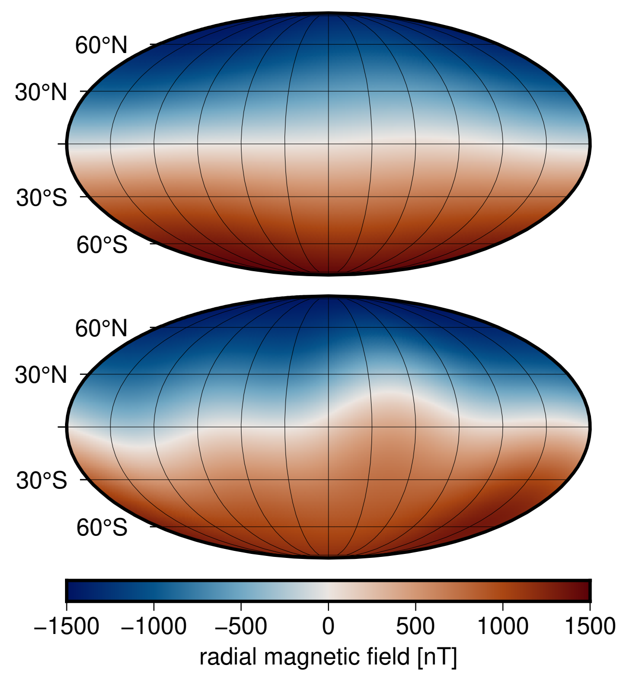

Figure 3: Radial component of Ganymede's core magnetic field evaluated on the surface $R = 2631.2$ km. Top: Model I. Bottom: Model II.

References

[1] Kivelson M. G. et al. (2002). *Icarus*, 157, 507–522. [2] Weber T. et al. (2021). *AGU Fall Meeting 2021*, SM51C-04. [3] Zhan X. and Schubert G. (2012). *JGR*, 117, E09011. [4] Breuer D. et al. (2015). *PEPI*, 2:39 [5] Christensen U. (2015). *Icarus*, 247, 248–259. [6] Johnson C. L. et al. (2018). ISBN: 9781107154452, pages: 115–143. [7] Acton C. H. (1996). *PSS* 4(1), 65–70. [8] Annex et al. (2020). *J. Open Source Software*, 5(46), 2050. [9] Voorhies et al. (2002). *JGR*, 107(E6), 5034.